

Efficient Joint Resource Allocation for Wireless Powered ISAC with Target Localization

Boyao Li[†], Qinwei He[‡], Boao Zhang[†], Xiaopeng Yuan^{†*} and Anke Schmeink[†]

[†]INDA Institute, RWTH Aachen University, Germany, Email: li|zhang|yuan|schmeink@inda.rwth-aachen.de

[‡]Global Energy Interconnection Research Institute Europe GmbH, Germany, Email: qinwei.he@geiri.eu

Abstract—Wireless powered integrated sensing and communication (ISAC) faces a fundamental tradeoff between energy supply, communication throughput, and sensing accuracy. This paper investigates a wireless powered ISAC system with target localization requirements, where users harvest energy from wireless power transfer (WPT) and then conduct ISAC transmissions in a time-division manner. In addition to energy supply, the WPT signal also contributes to target sensing, and the localization accuracy is characterized by Cramér-Rao bound (CRB) constraints. Under this setting, we formulate a max-min throughput maximization problem by jointly allocating the WPT duration, ISAC transmission time allocation, and transmit power. Due to the nonconvexity of the resulting problem, a suitable reformulation is developed by exploiting variable substitutions and the monotonicity of logarithmic functions, based on which an efficient successive convex approximation (SCA)-based iterative algorithm is proposed. Simulation results demonstrate convergence and significant performance gains over benchmark schemes, highlighting the importance of coordinated time-power optimization in balancing sensing accuracy and communication performance in wireless powered ISAC systems.

Index Terms—Integrated sensing and communication (ISAC), wireless power transfer (WPT), Cramer-Rao bound (CRB), resource allocation.

I. INTRODUCTION

Integrated sensing and communication (ISAC) has emerged as a key pillar of 6G wireless networks, enabling high-quality wireless connectivity and accurate sensing capability within a unified infrastructure [1]. By sharing spectrum, hardware, and waveforms, ISAC is expected to support a variety of emerging applications such as smart home, human-computer interaction, and vehicle-to-everything (V2X) [2]. This tight integration, however, also introduces fundamental tradeoffs between sensing and communication, since both functionalities must share limited resources to satisfy heterogeneous performance requirements.

As one of the two core functionalities of ISAC, sensing can be broadly categorized into three task types: detection, estimation, and recognition [3]. Detection-oriented sensing aims to determine the presence or absence of a target, whereas recognition focuses on identifying the target category or event type. In contrast, estimation aims to extract parameters of interest, e.g., angle, velocity, or location of the sensed object,

and has become increasingly attractive in both academia and industry. Estimation performance is commonly quantified by the mean squared error (MSE), defined as the expected squared difference between the true and estimated parameters. When the exact MSE is difficult to obtain, an informative alternative is the Cramér-Rao bound (CRB), which provides a lower bound on the error variance achievable by unbiased estimators. In particular, for target localization, the CRB is widely adopted to characterize the attainable positioning accuracy [4], since it explicitly captures the impact of sensing geometry.

Despite its potential, practical ISAC deployments are often constrained by limited energy supply, as many ISAC devices, e.g., sensors and edge nodes, are powered by finite-capacity batteries. Wireless power transfer (WPT) has therefore been introduced as a promising solution to enable sustainable ISAC operation by replenishing energy at energy-constrained devices [5], [6]. In WPT-enabled ISAC systems, efficient resource allocation is crucial to balance sensing accuracy and communication throughput so as to fully exploit the harvested energy. In [7], the authors jointly optimize power allocation and beamforming in a wirelessly powered ISAC framework. However, the WPT/ISAC durations are fixed, and the WPT phase is used purely for energy delivery without contributing to sensing, leaving the potential gains from time optimization and WPT-sensing co-design unexplored. Along a different line, [8] studied UAV-enabled WPT-assisted ISAC with TDMA-based time scheduling and joint resource optimization, while characterizing sensing performance via a SINR metric, which is insufficient for target localization.

To fill this gap, we study a wireless powered ISAC system in which the WPT signal is exploited not only for energy delivery but also for sensing, and formulate a joint optimization problem to maximize the minimum user throughput by optimizing the WPT duration, ISAC time allocation, and transmit power under energy causality and CRB-based sensing accuracy constraints. The main contributions of this paper are summarized as follows:

- We propose a wireless powered ISAC framework specialized for target localization, where the WPT phase is exploited for both energy transfer and sensing, and the localization accuracy is explicitly guaranteed via CRB

*X. Yuan is the corresponding author.

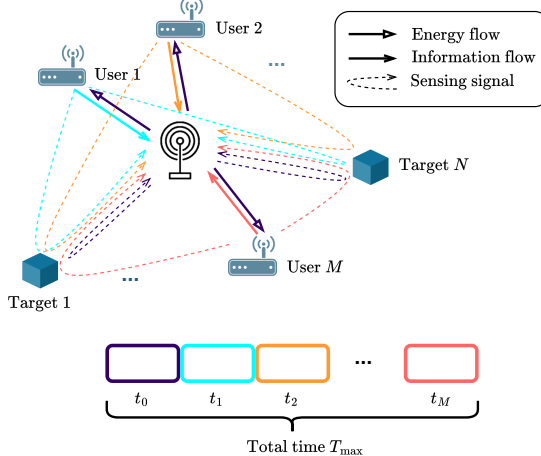


Fig. 1. Illustration of a wireless powered M -user ISAC system with N sensing targets.

constraints.

- To make the resulting nonconvex problem more tractable, we first introduce variable transformations and exploit the monotonicity of logarithmic functions to simplify the original coupling structure. Building on this reformulation, we address the remaining nonconvexity through convex approximation, resulting in an effective iterative algorithm that yields a high-quality suboptimal solution.
- Simulation results verify that the proposed joint optimization scheme significantly outperforms benchmark schemes, highlighting the importance of coordinated time and power allocation in WPT-enabled ISAC systems.

The rest of this paper is organized as follows. In Section II, we introduce the system model and formulate the optimization problem. Section III develops the proposed iterative algorithm. Numerical results are presented in Section IV, and conclusions are drawn in Section V.

II. PROBLEM FORMULATION

We consider a wireless powered ISAC system consisting of M users, N passive targets, and a base station (BS) located at $\mathbf{x}_0 \in \mathbb{R}^2$, as shown in Fig. 1. The position of user $m \in \mathcal{M} \triangleq \{1, \dots, M\}$ is denoted by $\mathbf{x}_m \in \mathbb{R}^2$, while the position¹ of target $n \in \mathcal{N} \triangleq \{1, \dots, N\}$ is denoted by $\mathbf{q}_n \in \mathbb{R}^2$.

In the first phase, the BS broadcasts an energy-carrying waveform with fixed power p_0 over a duration t_0 , from which all users harvest energy for subsequent ISAC transmissions. The amount of energy harvested by user m can be expressed as a function of t_0 :

$$E_m(t_0) = \zeta_m h_{0,m} t_0 p_0, \quad \forall m \in \mathcal{M}, \quad (1)$$

where ζ_m is the energy conversion efficiency of user m and $h_{0,m}$ denotes the channel gain from the BS to user m .

¹Here, the position refers to a reference target point corresponding to a preliminary location estimate, which is assumed to be available from prior sensing results.

After the wireless power transfer (WPT) phase, the system enters an ISAC phase consisting of M time slots. In slot m , user m transmits an information-bearing waveform with power p_m over a duration t_m , which simultaneously supports target sensing and uplink communication. The total transmission duration, including the wireless power transfer phase t_0 and the ISAC transmission phase t_m , $\forall m \in \mathcal{M}$ is constrained by a maximum total time budget T_{\max} , i.e.,

$$\sum_{m=0}^M t_m \leq T_{\max}. \quad (2)$$

Since the transmission of user m is solely powered by the harvested energy $E_m(t_0)$, the following energy causality constraint must hold:

$$t_m p_m \leq E_m(t_0), \quad \forall m \in \mathcal{M}. \quad (3)$$

Furthermore, due to hardware limitations, the transmit power of each user is bounded by

$$0 < p_m \leq P_{\max}, \quad \forall m \in \mathcal{M}. \quad (4)$$

The transmitted signal illuminates all passive targets, which then backscatter the incident energy toward the BS. The BS receives the composite scatter signal and performs bistatic sensing to infer target positions. This slot-by-slot illumination structure enables each user to contribute to the sensing process while operating under its individual energy budget harvested from the BS.

For each target $n \in \mathcal{N}$, we characterize the bistatic sensing geometry. The bistatic round-trip distance is given by

$$r_{m,n} = \|\mathbf{x}_m - \mathbf{q}_n\| + \|\mathbf{x}_0 - \mathbf{q}_n\|, \quad \forall m \in \mathcal{M}, \quad \forall n \in \mathcal{N}. \quad (5)$$

In addition to the user transmissions, the energy-carrying signal transmitted by the BS also illuminates the target and therefore contributes to sensing. The corresponding monostatic round-trip distance is given by

$$r_{0,n} = 2\|\mathbf{x}_0 - \mathbf{q}_n\|, \quad \forall n \in \mathcal{N}. \quad (6)$$

For each $n \in \mathcal{N}$, taking the gradient of $r_{m,n}$ with respect to the target location \mathbf{q}_n yields

$$\nabla_{\mathbf{q}_n} r_{m,n} = \begin{cases} -\frac{\mathbf{x}_m - \mathbf{q}_n}{\|\mathbf{x}_m - \mathbf{q}_n\|} - \frac{\mathbf{x}_0 - \mathbf{q}_n}{\|\mathbf{x}_0 - \mathbf{q}_n\|}, & m \in \mathcal{M}, \\ -2\frac{\mathbf{x}_0 - \mathbf{q}_n}{\|\mathbf{x}_0 - \mathbf{q}_n\|}, & m = 0, \\ \triangleq \begin{bmatrix} X_{m,n} \\ Y_{m,n} \end{bmatrix}, & \forall m \in \mathcal{M} \cup \{0\}, \quad \forall n \in \mathcal{N}. \end{cases} \quad (7)$$

Following the classical CRB analysis for range-based target localization [4], [9], the Fisher information matrix (FIM) associated with target n can be expressed as

$$\mathbf{J}_n = \sum_{m=0}^M p_m K_{m,n} \begin{bmatrix} X_{m,n}^2 & X_{m,n} Y_{m,n} \\ X_{m,n} Y_{m,n} & Y_{m,n}^2 \end{bmatrix}, \quad \forall n \in \mathcal{N}, \quad (8)$$

where the coefficient is defined as

$$K_{m,n} = \frac{8\pi^2 W^2 h_{m,n}}{\sigma^2 c^2}, \quad \forall m \in \mathcal{M} \cup \{0\}, \quad \forall n \in \mathcal{N}, \quad (9)$$

where W denotes the effective bandwidth, $h_{m,n}$ denotes the channel gain from transmitter m to target n , with $m = 0$ corresponding to the BS and $m \in \mathcal{M}$ corresponding to the users. σ^2 is the noise power at the BS receiver and c is the speed of light.

For notational convenience, the FIM associated with target n is rewritten in a compact form as

$$\mathbf{J}_n = \begin{bmatrix} A_n & C_n \\ C_n & B_n \end{bmatrix}, \quad \forall n \in \mathcal{N}, \quad (10)$$

where

$$A_n = \sum_{m=0}^M p_m K_{m,n} X_{m,n}^2, \quad (11)$$

$$B_n = \sum_{m=0}^M p_m K_{m,n} Y_{m,n}^2, \quad (12)$$

$$C_n = \sum_{m=0}^M p_m K_{m,n} X_{m,n} Y_{m,n}. \quad (13)$$

Under non-degenerate sensing geometry, the FIM is positive definite, i.e., $A_n B_n - C_n^2 > 0$, the Cramér-Rao bound (CRB) matrix can be expressed as the inverse of \mathbf{J}_n :

$$\mathbf{J}_n^{-1} = \frac{1}{A_n B_n - C_n^2} \begin{bmatrix} B_n & -C_n \\ -C_n & A_n \end{bmatrix}, \quad \forall n \in \mathcal{N}. \quad (14)$$

The trace of CRB matrix represent a lower bound on the sum of the MSEs for the target location estimation, which is calculated as

$$\text{tr}(\mathbf{J}_n^{-1}) = \frac{A_n + B_n}{A_n B_n - C_n^2}, \quad \forall n \in \mathcal{N}. \quad (15)$$

Given a predetermined target localization accuracy $\eta > 0$, the following constraint must be satisfied:

$$\text{tr}(\mathbf{J}_n^{-1}) \leq \eta, \quad \forall n \in \mathcal{N}. \quad (16)$$

Since $A_n B_n - C_n^2 > 0$, the above inequality can be rewritten as

$$A_n + B_n - \eta(A_n B_n - C_n^2) \leq 0, \quad \forall n \in \mathcal{N}. \quad (17)$$

To reveal the algebraic structure of the term $A_n B_n - C_n^2$ and to explicitly expose its dependence on the power variables $\{p_m\}$, we define $k_m = \sqrt{p_m K_{m,n} X_{m,n}}$ and $b_m = \sqrt{p_m K_{m,n} Y_{m,n}}$. Then $A_n = \|\mathbf{a}\|^2$, $B_n = \|\mathbf{b}\|^2$, and

$C_n = \mathbf{a}^\top \mathbf{b}$. Hence, for all $n \in \mathcal{N}$,

$$\begin{aligned} & A_n B_n - C_n^2 \\ &= \|\mathbf{a}\|^2 \|\mathbf{b}\|^2 - (\mathbf{a}^\top \mathbf{b})^2 \\ &= \frac{1}{2} \sum_{i=0}^M \sum_{j=0}^M (a_i b_j - a_j b_i)^2 \\ &= \frac{1}{2} \sum_{i=0}^M \sum_{j=0}^M p_i p_j K_{i,n} K_{j,n} (X_{i,n} Y_{j,n} - X_{j,n} Y_{i,n})^2, \end{aligned} \quad (18)$$

where the second equality follows from a standard algebraic identity associated with the Cauchy-Schwarz inequality.

By substituting (18) and separating the terms involving the fixed BS power p_0 , the expression in (17) can be rearranged as

$$\begin{aligned} & A_n + B_n - \eta(A_n B_n - C_n^2) \\ &= \sum_{m=1}^M \alpha_{m,n} p_m + \mu_n - \frac{\eta}{2} \sum_{i=1}^M \sum_{j=1}^M \beta_{i,j,n} p_i p_j \\ &\quad - \eta p_0 \sum_{m=1}^M \varphi_{m,n} p_m \\ &\triangleq F_n(\mathbf{p}), \quad \forall n \in \mathcal{N}, \end{aligned} \quad (19)$$

where $\mathbf{p} \triangleq [p_1, \dots, p_M]^\top$ denotes the vector of transmit powers. The coefficients are defined as

$$\alpha_{m,n} \triangleq K_{m,n} (X_{m,n}^2 + Y_{m,n}^2), \quad m \in \mathcal{M}, \quad (20)$$

$$\mu_n \triangleq p_0 K_{0,n} (X_{0,n}^2 + Y_{0,n}^2), \quad (21)$$

$$\beta_{i,j,n} \triangleq K_{i,n} K_{j,n} (X_{i,n} Y_{j,n} - X_{j,n} Y_{i,n})^2, \quad i, j \in \mathcal{M}, \quad (22)$$

$$\varphi_{m,n} \triangleq K_{0,n} K_{m,n} (X_{0,n} Y_{m,n} - X_{m,n} Y_{0,n})^2, \quad m \in \mathcal{M}. \quad (23)$$

During the ISAC transmission phase, while illuminating the targets for sensing, user m simultaneously transmits its data to the BS. The received SNR at the BS is

$$\gamma_m(p_m) = \frac{p_m h_{0,m}}{\sigma^2}, \quad \forall m \in \mathcal{M}. \quad (24)$$

Under the Shannon capacity model, the achievable throughput of user m for a transmission duration t_m is expressed as

$$R_m(t_m, p_m) = t_m W \log_2(1 + \gamma_m(p_m)), \quad \forall m \in \mathcal{M}. \quad (25)$$

To maximize the communication performance while ensuring fairness among all users, the minimum achievable throughput is adopted as the optimization objective. Accordingly, the overall optimization problem is formulated as

$$(\mathcal{P}1): \max_{\mathbf{t}, \mathbf{p}} \min_{m \in \mathcal{M}} \{R_m(t_m, p_m)\} \quad (26a)$$

$$\text{s.t. } t_m > 0, \forall m \in \mathcal{M} \cup \{0\}, \quad (26b)$$

$$\sum_{m=0}^M t_m \leq T_{\max}, \quad (26c)$$

$$0 < p_m \leq P_{\max}, \forall m \in \mathcal{M}, \quad (26d)$$

$$t_m p_m \leq E_m(t_0), \forall m \in \mathcal{M}, \quad (26e)$$

$$F_n(\mathbf{p}) \leq 0, \forall n \in \mathcal{N}, \quad (26f)$$

where $\mathbf{t} \triangleq [t_0, t_1, \dots, t_M]^T \in \mathbb{R}^{M+1}$ collects the transmit durations of the BS and all users. Problem $(\mathcal{P}1)$ is nonconvex due to the nonconvex nature of both the objective function and the constraints. Specifically, the throughput function $R_m(t_m, p_m)$ is neither jointly concave nor jointly convex with respect to (t_m, p_m) , as indicated by its indefinite Hessian matrix. Moreover, constraints $(26e)$ and $(26f)$ involve multiplicative couplings among the optimization variables, which render them nonconvex. As a result, problem $(\mathcal{P}1)$ cannot be directly solved using standard convex optimization techniques.

III. PROPOSED ITERATIVE SOLUTION

A. Problem Reformulation

To address these challenges, we reformulate the problem in this section.

First, we introduce new optimization variables

$$u_m = \log(t_m), v_m = \log(p_m), \forall m \in \mathcal{M}, \quad (27)$$

which guarantees $t_m > 0$ and $p_m > 0$ automatically.

The throughput (25) transforms to

$$\begin{aligned} R_m(t_m, p_m) &= e^{u_m} W \log_2 \left(1 + \frac{h_{0,m}}{\sigma^2} e^{v_m} \right) \\ &\triangleq \tilde{R}_m(u_m, v_m), \forall m \in \mathcal{M}, \end{aligned} \quad (28)$$

which is neither jointly concave nor convex in (u_m, v_m) .

To overcome this difficulty, we apply a logarithmic transformation to $\tilde{R}_m(u_m, v_m)$. Since the logarithm is strictly increasing, maximizing $\tilde{R}_m(u_m, v_m)$ is equivalent to maximizing $\log \tilde{R}_m(u_m, v_m)$, which can be expressed as, $\forall m \in \mathcal{M}$,

$$\log \tilde{R}_m(u_m, v_m) = u_m + W \log \left(\log_2 \left(1 + \frac{h_{0,m}}{\sigma^2} e^{v_m} \right) \right). \quad (29)$$

The first term is linear in u_m , while the second term is a positive scaling of a concave function with respect to v_m .

Consequently, $\log \tilde{R}_m(u_m, v_m)$ is jointly concave in (u_m, v_m) , since it is the sum of a linear function in u_m and a concave function in v_m . Moreover, the objective function $\min_{m \in \mathcal{M}} \{\log \tilde{R}_m(u_m, v_m)\}$ remains concave, as the pointwise minimum of concave functions is also concave.

As for CRB constraint $(26f)$, we define $v_0 \triangleq \log(p_0)$ as a constant for notational convenience. By replacing the

Algorithm 1 Proposed Iterative Algorithm for $(\mathcal{P}1)$

Initialization

Initialize a feasible point $(t_0^{(1)}, \mathbf{u}^{(1)}, \mathbf{v}^{(1)})$, set iteration no. $r = 1$ and threshold λ_{th} .

Iteration

a) Build convex problem $(\mathcal{P}2^{(r)})$ on the feasible point $(t_0^{(r)}, \mathbf{u}^{(r)}, \mathbf{v}^{(r)})$;

b) Solve $(\mathcal{P}2^{(r)})$ and obtain the optimal solution $(t_0^{(r*)}, \mathbf{u}^{(r*)}, \mathbf{v}^{(r*)})$;

c) If the objective improvement is below the threshold λ_{th}
Define the final solution as $(t_0^*, \mathbf{u}^*, \mathbf{v}^*) = (t_0^{(r*)}, \mathbf{u}^{(r*)}, \mathbf{v}^{(r*)})$,
and go to d).

Else define $(t_0^{(r+1)}, \mathbf{u}^{(r+1)}, \mathbf{v}^{(r+1)}) = (t_0^{(r*)}, \mathbf{u}^{(r*)}, \mathbf{v}^{(r*)})$, $r = r + 1$,
and go back to a).

Reconstruction

d) Recover the original variables by $t_m^* = e^{u_m^*}$ and $p_m^* = e^{v_m^*}$, $\forall m \in \mathcal{M}$, and then calculate the optimum of $(\mathcal{P}1)$.

optimization variables, it can be compactly written as

$$\begin{aligned} F_n(\mathbf{p}) &= \sum_{m=1}^M \alpha_{m,n} e^{v_m} + \mu_n - \frac{\eta}{2} \sum_{i=1}^M \sum_{j=1}^M \beta_{i,j,n} e^{v_i + v_j} \\ &\quad - \eta p_0 \sum_{m=1}^M \varphi_{m,n} e^{v_m} \\ &\triangleq \tilde{F}_n(\mathbf{v}), \forall n \in \mathcal{N}. \end{aligned} \quad (30)$$

While the first two terms are convex in \mathbf{v} , the last two terms are the negative of convex functions, rendering $\tilde{F}_n(\mathbf{v})$ nonconvex.

Overall, the reformulated optimization problem is given by

$$(\mathcal{P}2): \max_{t_0, \mathbf{u}, \mathbf{v}} \min_{m \in \mathcal{M}} \{\log \tilde{R}_m(u_m, v_m)\} \quad (31a)$$

$$\text{s.t. } t_0 > 0, \quad (31b)$$

$$t_0 + \sum_{m=1}^M e^{u_m} \leq T_{\max}, \quad (31c)$$

$$v_m \leq \log P_{\max}, \forall m \in \mathcal{M}, \quad (31d)$$

$$u_m + v_m \leq \log(E_m(t_0)), \forall m \in \mathcal{M}, \quad (31e)$$

$$\tilde{F}_n(\mathbf{v}) \leq 0, \forall n \in \mathcal{N}, \quad (31f)$$

where $\mathbf{u} \triangleq [u_1, \dots, u_M]^T \in \mathbb{R}^M$ and $\mathbf{v} \triangleq [v_1, \dots, v_M]^T \in \mathbb{R}^M$. Compared with the original problem $(\mathcal{P}1)$, problem $(\mathcal{P}2)$ is considerably more tractable due to the concave objective function and affine constraints. Nevertheless, it remains nonconvex because of the nonconvex constraint $(31f)$. To tackle this issue, we construct suitable convex approximations and develop a successive convex approximation (SCA)-based solution framework in the following subsections [10].

B. Iterative Algorithm

To handle the nonconvexity in $(31f)$, we construct a convex upper bound using the first-order Taylor expansion at a local feasible point. Specifically, at the r -th iteration, we denote the current local feasible point as $\mathbf{v}^{(r)}$. Since $e^{v_i + v_j}$ is convex, its first-order Taylor approximation at $(v_i^{(r)}, v_j^{(r)})$ provides a global lower bound. Consequently, the negative of this term yields an affine upper bound for the nonconvex part of $(31f)$.

The resulting convex upper bound is denoted by $\tilde{F}_n^{(r)}(\mathbf{v})$ in (32) at the top of the next page.

$$(\mathcal{P}2^{(r)}): \max_{t_0, \mathbf{u}, \mathbf{v}} \min_{m \in \mathcal{M}} \{\log \tilde{R}_m(u_m, v_m)\} \quad (33a)$$

$$\text{s.t. } t_0 > 0, \quad (33b)$$

$$t_0 + \sum_{m=1}^M e^{u_m} \leq T_{\max}, \quad (33c)$$

$$v_m \leq \log P_{\max}, \forall m \in \mathcal{M}, \quad (33d)$$

$$u_m + v_m \leq \log(E_m(t_0)), \forall m \in \mathcal{M}, \quad (33e)$$

$$\tilde{F}_n^{(r)}(\mathbf{v}) \leq 0, \forall n \in \mathcal{N}, \quad (33f)$$

which is a convex optimization problem and can be easily solved using convex optimization tools. Also, the inequality in (32) makes sure that the constraint (33f) is always stricter than (31f), thus the feasible point in $(\mathcal{P}2^{(r)})$ is always feasible in $(\mathcal{P}2)$. The overall SCA-based iterative procedure that successively solves $(\mathcal{P}2^{(r)})$ is summarized in Algorithm 1.

IV. NUMERICAL RESULTS

In this section, numerical results are presented to evaluate the performance of the proposed wireless powered ISAC system. We consider a wireless powered ISAC system consisting of one BS, $M = 10$ users, and $N = 10$ passive targets, where the BS is located at the origin and users as well as targets are randomly and independently distributed over a circular area of radius 10 m centered at the BS. The wireless channel gain between any pair of nodes follows a distance-dependent path-loss model given by $h = z\kappa d^{-\nu}$, where d denotes the Euclidean distance, $\kappa = 10^{-3}$ is the path-loss constant, $\nu = 2.5$ is the path-loss exponent, and z represents a small-scale fading coefficient modeled as an independent Rayleigh-distributed random variable. Unless otherwise stated, the default simulation parameters are set as follows: $c = 3 \times 10^8$ m/s, $T_{\max} = 10$ s, $p_0 = 10$ W, $P_{\max} = 2$ W, $\sigma^2 = -70$ dBm, $\eta = 5 \times 10^{-2}$, $W = 1$ MHz, $\zeta_m = 0.7$, $\forall m \in \mathcal{M}$, and $\lambda_{\text{th}} = 10^{-5}$.

To further demonstrate the effectiveness of the proposed joint time-power allocation scheme, we consider the following two benchmark schemes for performance comparison:

- *Equal ISAC Time*: The total ISAC transmission duration is equally divided among all users, i.e., $t_m = t$, $\forall m \in \mathcal{M}$. The energy harvesting duration t_0 , the common ISAC transmission time t , and the transmit power \mathbf{p} are jointly optimized using the iterative algorithm.
- *Maximum Transmit Power*: All users transmit with the maximum allowable power, i.e., $p_m = P_{\max}$, $\forall m \in \mathcal{M}$, while the energy harvesting duration t_0 and the ISAC transmission durations \mathbf{t} are jointly optimized using a similar iterative algorithm.

The simulation results are obtained based on a random realization of the ISAC system. We first examine the convergence behavior of the proposed iterative algorithm. Fig. 2

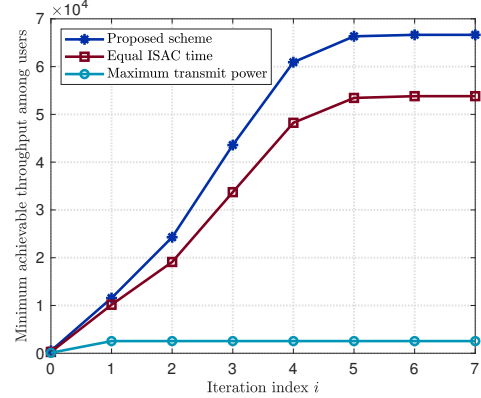


Fig. 2. Convergence behavior of the proposed and benchmark schemes.

illustrates the evolution of the minimum achievable throughput among users versus the iteration index. It is observed that the proposed algorithm converges rapidly and stabilizes within a few iterations, demonstrating its reliability and efficiency. Compared with the benchmark schemes, the proposed method consistently achieves a higher throughput during the convergence process.

Fig. 3 depicts the minimum achievable throughput as a function of the target localization accuracy requirement η . As η increases, corresponding to a relaxed sensing constraint, the achievable throughput of all schemes improves. The proposed method outperforms the benchmark schemes over the entire range of η , highlighting the benefit of jointly optimizing the energy harvesting duration, ISAC transmission time, and transmit power. In contrast, the fixed maximum transmit power scheme yields limited performance gains, indicating that simply increasing transmit power is insufficient to effectively balance sensing and communication requirements.

Fig. 4 shows the minimum achievable throughput among users as a function of the WPT transmit power p_0 . As p_0 increases, the achievable throughput of all schemes improves monotonically, since more energy can be harvested to support ISAC transmissions. The proposed method consistently outperforms the benchmark schemes over the entire range of p_0 , demonstrating the benefit of jointly optimizing the energy harvesting duration, ISAC transmission time, and transmit power. In contrast, the equal ISAC time scheme exhibits inferior performance due to its limited flexibility in time allocation. Moreover, the fixed maximum transmit power scheme achieves only marginal throughput gains, indicating that increasing WPT power alone is insufficient to fully exploit the sensing and communication tradeoff under the sensing constraints.

V. CONCLUSION

This paper investigated a wireless powered ISAC system with CRB-based target localization requirements. By explicitly incorporating sensing accuracy constraints into the resource allocation design, a joint time-power optimization problem was formulated to maximize the minimum achievable throughput among users under energy harvesting and power

$$\begin{aligned}
\tilde{F}_n(\mathbf{v}) \leq & \sum_{m=1}^M \alpha_{m,n} e^{v_m} + \mu_n - \frac{\eta}{2} \sum_{i=1}^M \sum_{j=1}^M \beta_{i,j,n} e^{v_i^{(r)} + v_j^{(r)}} \left[1 + (v_i - v_i^{(r)}) + (v_j - v_j^{(r)}) \right] \\
& - \eta p_0 \sum_{m=1}^M \varphi_{m,n} e^{v_m^{(r)}} \left[1 + (v_m - v_m^{(r)}) \right] \triangleq \tilde{F}_n^{(r)}(\mathbf{v}), \forall n \in \mathcal{N}
\end{aligned} \tag{32}$$

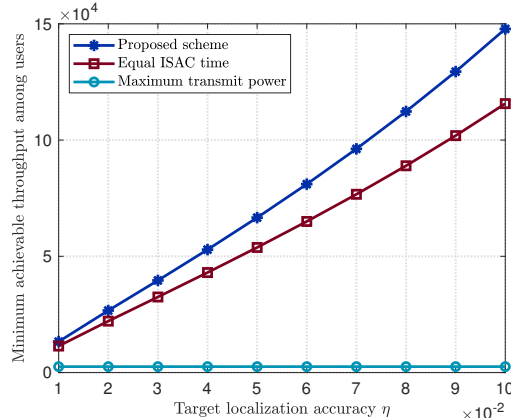


Fig. 3. Minimum achievable throughput versus target localization accuracy.

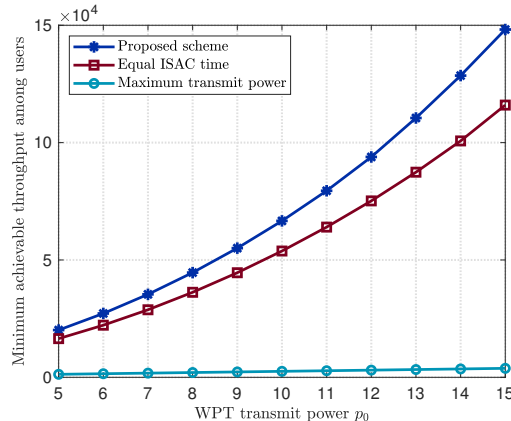


Fig. 4. Minimum achievable throughput versus WPT transmit power.

constraints. Due to the nonconvex nature of the problem, an efficient iterative algorithm based on successive convex approximation was developed.

Simulation results demonstrated that the proposed algorithm converges rapidly and significantly outperforms benchmark schemes, including equal ISAC time allocation and fixed maximum transmit power strategies. The results further revealed that blindly increasing transmit power is insufficient to achieve an effective balance between sensing accuracy and communication performance, highlighting the importance of coordinated time and power allocation in wireless powered ISAC systems.

REFERENCES

- [1] S. Lu et al., “Integrated Sensing and Communications: Recent Advances and Ten Open Challenges,” *IEEE Internet Things J.*, vol. 11, no. 11, pp. 19094-19120, Jun. 2024.
- [2] Y. Cui, F. Liu, X. Jing and J. Mu, “Integrating Sensing and Communications for Ubiquitous IoT: Applications, Trends, and Challenges,” *IEEE Netw.*, vol. 35, no. 5, pp. 158-167, Sep. 2021.
- [3] F. Liu et al., “Integrated Sensing and Communications: Toward Dual-Functional Wireless Networks for 6G and Beyond,” *IEEE J. Sel. Areas Commun.*, vol. 40, no. 6, pp. 1728-1767, Jun. 2022.
- [4] H. Godrich, A. P. Petropulu and H. V. Poor, “Power Allocation Strategies for Target Localization in Distributed Multiple-Radar Architectures,” *IEEE Trans. Signal Process.*, vol. 59, no. 7, pp. 3226-3240, Jul. 2011.
- [5] X. Li et al., “Integrating Sensing, Communication, and Power Transfer: From Theory to Practice,” *IEEE Commun. Mag.*, vol. 62, no. 9, pp. 122-127, Sep. 2024.
- [6] Y. Chen, Z. Ren, J. Xu, Y. Zeng, D. W. K. Ng and S. Cui, “Integrated Sensing, Communication, and Powering: Toward Multi-Functional 6G Wireless Networks,” *IEEE Commun. Mag.*, vol. 63, no. 8, pp. 146-153, Aug. 2025.
- [7] X. Li, Z. Han, Z. Zhou, Q. Zhang, K. Huang, and Y. Gong, “Wirelessly powered integrated sensing and communication,” in *Proc. 1st ACM MobiCom Workshop ISCS*, Sydney, Australia, 2022, pp. 1-6.
- [8] O. Rezaei, M. M. Naghsh, S. M. Karbasi and M. M. Nayebi, “Resource Allocation for UAV-Enabled Integrated Sensing and Communication (ISAC) via Multi-Objective Optimization,” in *Proc. IEEE Int. Conf. Acoust., Speech Signal Process. (ICASSP)*, Rhodes Island, Greece, 2023, pp. 1-5.
- [9] H. Godrich, A. Petropulu and H. V. Poor, “Power allocation schemes for target localization in widely distributed MIMO radar systems,” in *Proc. IEEE Mil. Commun. Conf. (MILCOM)*, San Jose, CA, USA, 2010, pp. 846-851.
- [10] G. Scutari and Y. Sun, “Parallel and Distributed Successive Convex Approximation Methods for Big-Data Optimization,” in *Multi-Agent Optimization*. Cham, Switzerland: Springer, Jan. 2018, pp. 141-308.